UCRL-JC-150195

LAWRENCE
LIVERMORE
NATIONAL
LABORATORY

Hydrodynamic Instability of Ionization Fronts in HII Regions

A. Mizuta, J. Kane, D. Ryutov, B. Remington, H. Takabe, M. Pound

August 21, 2003

2003 Third International Conference on Inertial Fusion Sciences and Applications, Monterey, California, September 7-12, 2003

TuO6.4

HYDRODYNAMIC INSTABILITY OF IONIZATION FRONTS IN HII REGIONS

Akira Mizuta[1,2,4], Jave Kane[2], Dmitri Ryutov[2], Bruce Remington,[2], Hidekai Takabe[1], and Marc Pound[3]

1.Institute of Laser Engineering, Osaka University Yamada-Oka 2-6, Suita, Osaka, 565-0871, Japan

2.University of California, Lawrence Livermore National Laboratory

7000 East Ave., Livermore, CA, 94551

3. University of Maryland, College Park, MD 20742

4. amizuta@ile.osaka-u.ac.jp

Abstract

We investigate hydrodynamic instability of accelerating ionization fronts with two dimensional hydrodynamic simulations. When recombination in the ionized region is turned off, Rayleigh-Taylor instability is effective. Perturbation grows up with classical Rayleigh-Taylor growth rate. In the case with recombination, the local difference of absorption profile works to smooth the surface. The perturbation does not grow and the amplitude follows a damped oscillations with time .

I. INTRODUCTION

Ionization fronts near massive stars which are referred to O- or B-stars have attracted considerable interest due to their amazing shape. For example, the Eagle Nebula has three famous pillars or elephant trunks [1, 2]. Strong UV radiation from O, B-stars buries into the molecular surface and photoevaporation occurs in a very thin layer. As a result, an ablation flow begins. A shock propagates into the molecular cloud. Such an ionization or ablation front is categorized as D-type. The site is also known as a star formation region. Some young stellar objects and Herbig-Halo jets are observed in the nebula[3, 4]. It is important to study the formation of pillars to better understand the nebula and star formation theory.

A number of theoretical works and numerical simulations to understand the formation of pillars have been done so far. But this problem is still under discussion. Vandervoort [5] found instabilities of IF in a non-accelerating frame. Axford [6] extended it with the recombination case and concluded that recombination in the ionized gas works to smooth the surface when the wavelength of the perturbation is much larger than recombination length. Spitzer [7] proposed a model of Rayleigh-Taylor instability. Williams et al.[8] showed robust development of phtoionized columns with an isothermal model.

II. BASIC EQUATIONS

We solve two dimensional hydrodynamic equations with energy sources caused by radiative processes.

$$\frac{\partial \rho}{\partial t} + \nabla \cdot (\rho \boldsymbol{u}) = 0, \qquad (1)$$

$$\frac{\partial (\rho \boldsymbol{u})}{\partial t} + \nabla \cdot (\rho \boldsymbol{u}\boldsymbol{u} + \boldsymbol{P}) = 0, \qquad (2)$$

$$\frac{\partial}{\partial t}\left(\rho\left(\frac{1}{2}\boldsymbol{u}^2 + \epsilon\right)\right) + \nabla \cdot \left(\left(\rho\left(\frac{1}{2}\boldsymbol{u}^2 + \epsilon\right) + p\right)\boldsymbol{u}\right) = -q_{re} + q_{uv} - q_{mol}, \qquad (3)$$

where ρ is mass density, p is pressure, $\boldsymbol{u}$ is velocity vector, ϵ is specific internal energy, and n is volume density of total hydrogen respectively. q_{re}, q_{uv}, and q_{mol} are energy source terms due to recombination in the ionized region, absorption of UV radiation from O-stars, and cooling in the molecular gas. When a shock propagates into the molecular gas, the gas is radiatively cooled in a very short time scale[9].

Photoionization and recombination is considered with the following equations,

$$n\frac{\partial f}{\partial t} + n\boldsymbol{u}\cdot\nabla f = an(1-f)J - \alpha_B n^2 f^2, \tag{4}$$

$$\frac{\partial J}{\partial y} = -an(1-f)J, \tag{5}$$

where n_i is ionized hydrogen volume density, $f = n_i/n$ is ionization fraction, $a = 6\times10^{-18}\text{cm}^2$ is photoionization cross-section of hydrogen, and J is the number flux of ionizing photons which have the energy more than the critical energy (13.6eV). We do not include the recombination to ground state assuming diffuse radiation and its absorption are balanced locally (on the spot approximation). Only the case B recombination ($\alpha_B = 2.6\times10^{-13}\text{cm}^3\text{s}^{-1}$ at $T = 10^4$K [10]) is considered in this study. Energy sources are written as:

$$q_{re} = (nf)^2\beta_B k_B T, \tag{6}$$

$$q_{uv} = Wna(1-f)J, \tag{7}$$

$$q_{mol} = n_{mol}^2 \times 10^{-29}\text{erg cm}^{-3}\text{s}^{-1}, \tag{8}$$

$$T = \frac{m_p}{k_b}\frac{4\epsilon}{7f+5}, \tag{9}$$

$$n_{mol} = n(1-f)/2. \tag{10}$$

where T is temperature, m_p is proton mass, and k_b is Boltzmann constant. We use $\beta_B k_b T$ instead of $(3/2)k_b T$ for the recombination cooling term to include the effects of the thermal velocity dependence for the recombination and free-free coliisional cooling. $\beta_B = 1.25\alpha_B$ at $T = 10^4$ K[10]. It is assumed that the averaged energy of the photon is $(13.6 + W)$ eV per photon from O stars. The energy W is deposited to internal energy of the gas. The ionized region becomes isothermal quickly due to the energy balance between these cooling and heating effect. We take $W = 1.73\times10^{-12}$ erg to have isothermal temperature $T = 10^4$ K. The cooling term q_{mol} is effective with $40\text{K} < T < 3000\text{K}$.

To close the equations we also solve the equation of state:

$$p = \frac{2(3f+1)}{7f+5}\rho\epsilon + p_M\left(\frac{\rho}{\rho_M}\right)^{\gamma_M}. \tag{11}$$

The first term in the right hand side is thermal pressure and the second one is magnetic pressure. p_M, and ρ_M are constant values. The index is also constant $\gamma_M = 4/3$(magnetic turbulence) or 2(initially uniform magnetic field). This magnetic pressure is introduced to prevent radiative collapse due to molecular cooling when the shock heating occurs[11].

Then we get the sound speed,

$$\begin{aligned} c_s^2 &= \left(\frac{\partial p}{\partial\rho}\right)_\epsilon + \frac{p}{\rho^2}\left(\frac{\partial p}{\partial\epsilon}\right)_\rho \\ &= \frac{2(3f+1)}{7f+5}\left(\frac{p}{\rho}+\epsilon\right) + \frac{\gamma_M p_M}{\rho}\left(\frac{\rho}{\rho_M}\right)^{\gamma_M}. \end{aligned} \tag{12}$$

The hydodynamic equations are solved with a Godunov-type scheme code. The numerical scheme is the as same as used in Mizuta et al.[12], expendable to accept real gas equation of state is done[14]. Phtoionization and recombination in Eq. 4 and 5 are solved implicitly at both half and full step[13].

III. NUMERICAL CONDITIONS

We use two dimensional plane geometry (x-y). The grid size is uniform ($\Delta x = \Delta y = 2.5\times10^{-3}\text{pc} \sim 7.5\times10^{15}\text{cm}$ which is still longer than the mean free path of the incident photon for the molecular cloud).

Initially a quarter pc thick cloud is set 0.5pc away from the boundary where incident photon is introduced. The cloud has initial hydrogen number density $n(H) = 10^5\text{cm}^{-3}$ and temperature $T = 40$ K. A ionized gas is put between the boundary and the cloud surface. The number density is $n(H) = 10\text{cm}^{-3}$ and the gas is pressure matched with the molecular cloud. Behind the cloud a dilute molecular gas is put ($n(H) = 10\text{cm}^{-3}$ and $T = 40$K). Constant parameters p_M and ρ_M are chosen as same as thermal pressure and mass density of the initial molecular cloud. In this paper we concentrate $\gamma_M = 4/3$ case. The photon flux is parallel to y-axis and constant except for a short imprinting period.All of the gaseous are at rest at $t = 0$ when the radiative flux is turned on.

The dynamics is divided into three phases. At first, an ablation flow begins and a shock propagates into the molecular cloud (I). The velocity of the ablation front is almost constant in this period. When the shock breaks out the back side of the cloud a rarefaction appears and proceeds to the ablation front(II). Then the rarefaction arrives at the ablation front, and the accelerating phase begins(III).

A perturbation is imprinted by photon number flux for 10 kyr when phase III begins. The perturbation is a 10% sinusoidal amplitude in photon number flux, namely, $J = J_0(1 + 0.1\cos(2\pi x/\lambda))$, where

J_0 is constant photon number flux and λ is wave length. We studied three cases with different wave length ($\lambda = 0.92, 0.6,$ and 0.46 pc). We followed the evolution at least until the ablation front propagates the wavelength of the perturbation.

IV. RESULTS AND DISCUSSION

IV.A. Without Recombination

At first, we discuss the case without recombination, namely, $\alpha_B = \beta_B = 0$. Incident photon flux at the boundary is $|J_0| = 2.6 \times 10^9 \mathrm{cm}^{-2}\mathrm{s}^{-1}$. Figure 1 shows incident photon number flux (solid lines) and ablation front ($f = 0.5$) contour at $t = 340$ky. The absorption occurs in a very thin layer at the ablation front because of the very short mean free path of photons and no re-absorption in the ionized gas. Figure 2 shows the time evolution of amplitude of perturbation, where the amplitude is defined as the half thickness of $f = 0.5$ contour. Three wavelength cases are shown. The perturbation grows up in time in all cases and the growth rate is in good agreement with classical Rayleigh-Taylor theory[15] (the amplitude A is given; $A = A_0 \exp(\gamma t)$, where $\gamma = (kg)^{1/2}$ is the growth rate, $k = 2\pi/\lambda$ is wave number, and g is effective gravity derived from a one dimensional simulation without any perturbation. Atwood number is assumed to be unity.)

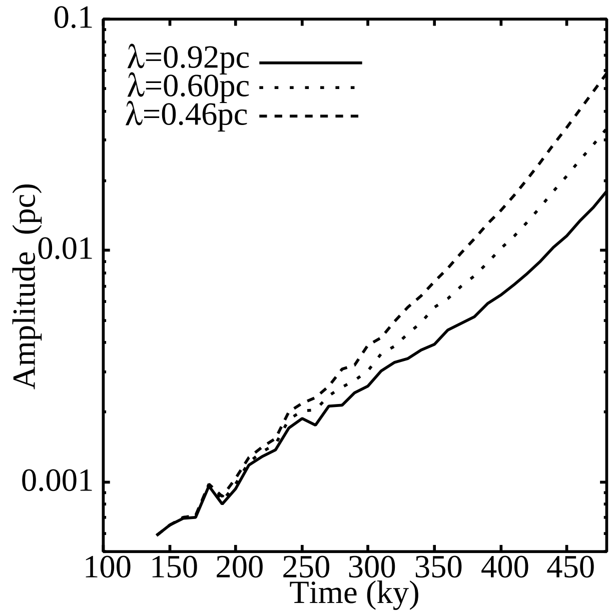

Fig.2 Time evolution of log scale amplitude of perturbation in each wavelength (without recombination case).

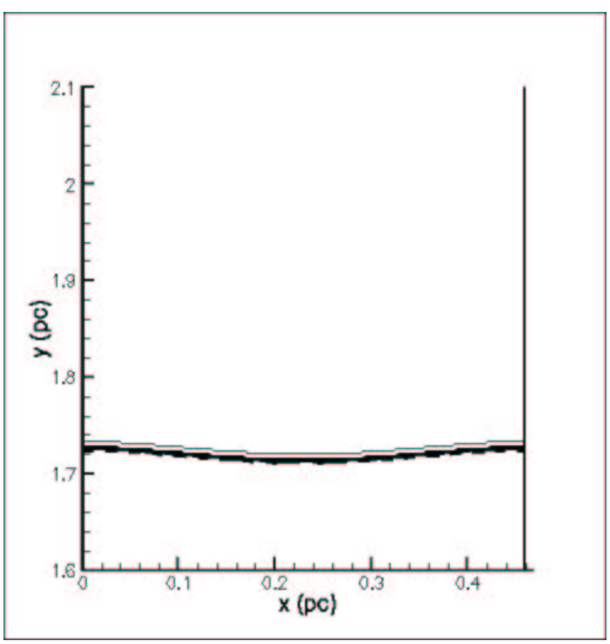

Fig.1 Photon number flux contour (solid lines), and ablation front ($f = 0.5$) contour (dashed line) at $t = 340$ky (without recombination case). Incident photon flux is incoming from up side (at y=3pc) to down side.

IV.B. With Recombination

On the contrary, in the case with recombination, the behavior of the imprinted perturbation is very different. The photon number flux is increased to $|J_0| = 5 \times 10^{11} \mathrm{cm}^{-2}\mathrm{s}^{-1}$ so that the effective gravity in accelerating phase is almost as same as the one in case without recombination. Figure 3 shows time evolution of the amplitude in three cases. The perturbation does not grow contrary to the case without recombination, and the amplitude is oscillating.

We can understand the reason why the perturbation does not grow as follows. Some of the ablated material in the bubble region converges and a dense region appears in the ionized gas near the ablation front (Fig.4). This density profile causes the difference of the absorption profile near the ablation front (Fig.5). In the dense gas the recombination rate is high, and absorption of incident photons is enhanced. The photon flux is larger around the spike, which is strongly driven or rocket effect is strong. On the other hand, incident photon is absorbed moderately around the bubble and rocket effect is weaker. As a result, the amplitude is reduced. Once the amplitude is reduced muti-mode patterns appear and oscillate but do not grow, contrary to the case without recombination.

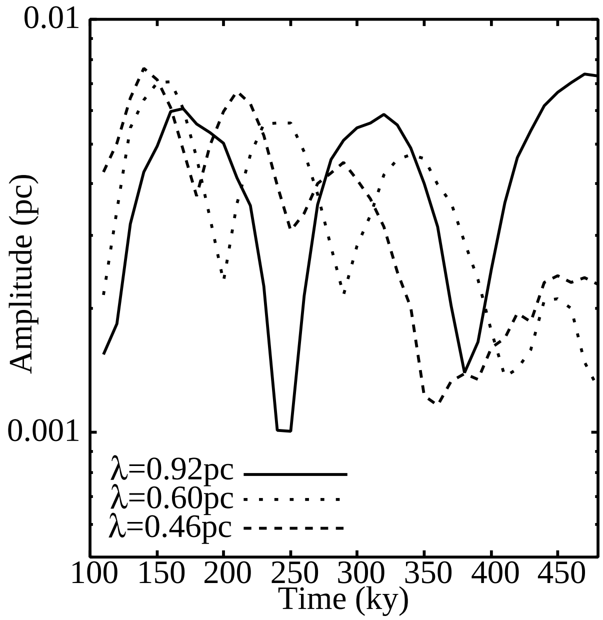

Fig.3 Same as Fig.2 (with recombination case).

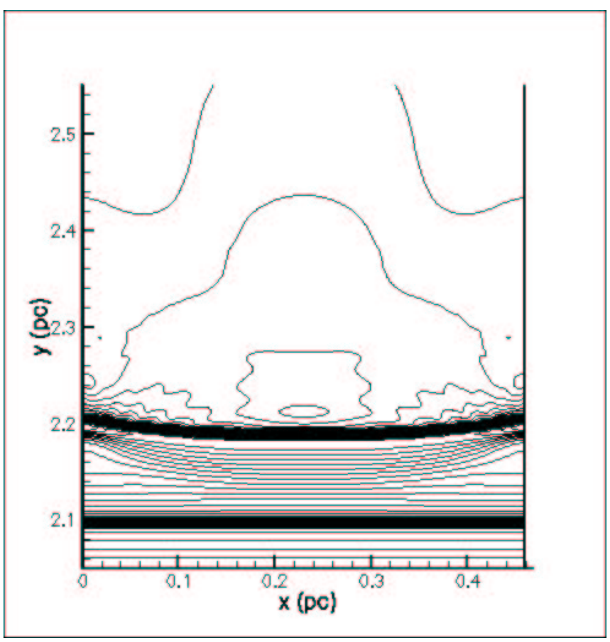

Fig.4 Log scale hydrogen number density contour at $t = 150$ky with recombination case Number density decreases away from the ablation front (see Fig.5).

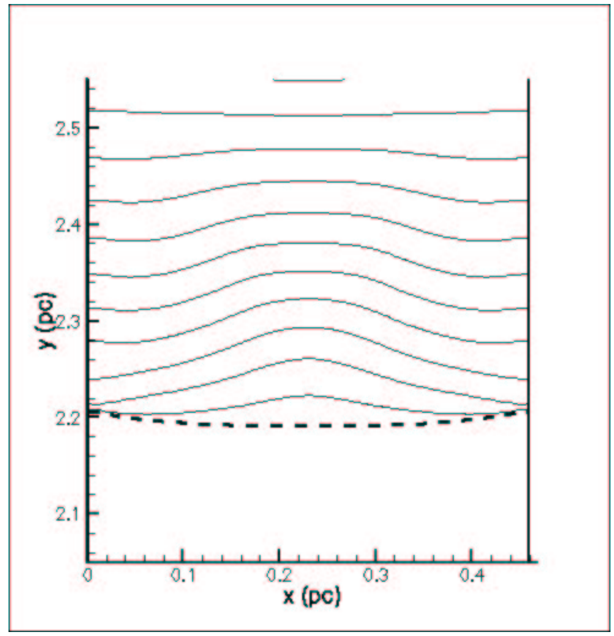

Fig.5 Photon number flux and ablation front contour (same as Fig.1) at the same time of Fig.4 with recombination case. Flux decreases from top to bottom.

V. CONCLUSION

Instabilities in ionization front are discussed with effective gravitation. The perturbation on the ionization front grows in the case without recombination. The growth rate is in good agreement with classical Rayleigh-Taylor instability. When recombination is turned on, which is the more realistic case, the difference of density profile causes a different absorption profile. This works to smooth the surface. The perturbation does not grow and the amplitude oscillates in time.

ACKNOWLEDGMENTS

We would like to thank Robin Williams for helpful discussions.

This work is performed under the auspices of the U.S. Department of Energy by the Lawrence Livermore National Laboratory under Contract No. W-7405-ENG-48 and NASA Grant NRA 00-01-ATP-059.

References

[1] J. HESTER, et al. Hubble Space Telescope WFPC2 Imaging of M16: Photoevaporation and Emerging Young Stellar Objects, *AJ*, **111**, 2349, 1996

[2] M. POUND, Molecular Gas in the Eagle Nebula, *ApJ*, L113, **493**, 1998

[3] M. POUND, B. REIPURTH, & J. BALLY, Looking into the Horshead, *AJ*, **125**, 2108, 2003

[4] J. BALLY, & B. REIPURTH, Irradiated Jets and Outflows in the Pelican Nebula, *AJ*, **126**, 893, 2003

[5] P. VANDERVOORT, On the Stability of Ionization Fronts, *ApJ*, **135**, 212, 1962

[6] W. AXFORD, The stability of Ionization Fronts, *ApJ*, **140**, 112, 1962

[7] L. SPITZER, Behavior of Matter In Space, *ApJ*, **120**, 1, 1954

[8] R. WILLIAMS, D. WARD-THOMPSON, & A. WHITWORTH, Hydrodynamics of Photoionized Columns in the Eagle Nebula, M 16, *MNRAS*, **327**, 788, 2001

[9] D. NEUFELD, S. LEPP, & G. MELNICK, Thermal Balance in Dense Molecular Clouds: Radiative Cooling Rates and Emission-Line Luminosities *ApJS*, **100**, 132, 1995

[10] D. HUMMER & M. SEATON, The Ionization Structure of Planetary Nebulae, I. Pure Hydrogen Nebulae, *MNRAS*, **125**, 437, 1963

[11] D. RYUTOV, & B. REMINGTON, Scaling Astrophysical Phenomena to High-Energy-Density Laboratory Experiments, *Plasma Phys. Controlled Fusion*, **44**, B407, 2002

[12] A. MIZUTA, S. YAMADA, & H. TAKABE, Numerical Analysis of Jets Produced by Intense Laser, *ApJ*, **567**, 635, 2002

[13] R. WILLIAMS, Shadowing Instabilities of Ionization Fronts, *MNRAS*, **310**, 789, 1999

[14] P. GLAISTER, Riemann Solvers with Primitive Parameter Vectors for Two-Dimensional Compressible Flows of a Real Gas, *COMP. MATH. APPLI.*, **126**, issue 2, 75, 1999

[15] S. CHANDRASEKHAR, *Hydrodynamic and Hydromagnetic Stability*, Chap. 10, Dover, New York, 1981